

# Tridiagonal test matrices for eigenvalue computations: two-parameter extensions of the Clement matrix<sup>1</sup>

Roy Oste, Joris Van der Jeugt

E-mail addresses: Roy.Oste@UGent.be, Joris.VanderJeugt@UGent.be

Department of Applied Mathematics, Computer Science and Statistics, Faculty of Sciences, Ghent University, Krijgslaan 281-S9, 9000 Gent, Belgium.

## Abstract

The Clement or Sylvester-Kac matrix is a tridiagonal matrix with zero diagonal and simple integer entries. Its spectrum is known explicitly and consists of integers which makes it a useful test matrix for numerical eigenvalue computations. We consider a new class of appealing two-parameter extensions of this matrix which have the same simple structure and whose eigenvalues are also given explicitly by a simple closed form expression. The aim of this paper is to present in an accessible form these new matrices and examine some numerical results regarding the use of these extensions as test matrices for numerical eigenvalue computations.

*Keywords:* Tridiagonal matrix; Exact eigenvalues; Eigenvalue computation; Clement matrix; Sylvester-Kac matrix

*2010 MSC:* 65F15; 15A18; 15A36

## 1 Introduction

For a positive integer  $n$ , consider the  $(n+1) \times (n+1)$  matrix  $C_n$  whose non-zero entries are given by

$$c_{k,k+1} = c_{n+2-k,n+1-k} = k \quad \text{for } k \in \{1, \dots, n\}, \quad (1)$$

or explicitly, the matrix

$$C_n = \begin{pmatrix} 0 & 1 & & & & & & & \\ n & 0 & 2 & & & & & & \\ & n-1 & 0 & 3 & & & & & \\ & & & \ddots & \ddots & \ddots & & & \\ & & & & 3 & 0 & n-1 & & \\ & & & & & 2 & 0 & n & \\ & & & & & & 1 & 0 & \end{pmatrix}. \quad (2)$$

This matrix appears in the literature under several names: the Sylvester-Kac matrix, the Kac matrix, the Clement matrix, etc. It was already considered by Sylvester [19], used by M. Kac in some of his seminal work [13], proposed by Clement as a test matrix for eigenvalue computations [5], and it continues to attract attention [20, 3, 2, 7].

The matrix  $C_n$  has a simple structure, it is tridiagonal with zero diagonal and has integer entries. The main property of  $C_n$  is that its spectrum is known explicitly and is remarkably simple; the eigenvalues of  $C_n$  are the integers

$$-n, -n+2, -n+4, \dots, n-2, n. \quad (3)$$

The  $n+1$  distinct eigenvalues are symmetric around zero, equidistant and range from  $-n$  to  $n$ . Hence for even  $n$ , they are  $n+1$  consecutive even integers, while for odd  $n$  they are  $n+1$  consecutive odd integers.

**Remark 1** *The eigenvectors of the matrix  $C_n$  are also known, they can be expressed in terms of the Krawtchouk orthogonal polynomials [16].*

---

<sup>1</sup>This is a preprint of a paper whose final and definite form is in Journal of Computational and Applied Mathematics: R. Oste, J. Van der Jeugt, Tridiagonal test matrices for eigenvalue computations: Two-parameter extensions of the Clement matrix, Journal of Computational and Applied Mathematics, **314** (2017), 30–39, ISSN 0377-0427, doi: <http://dx.doi.org/10.1016/j.cam.2016.10.019>.





**Lemma 1** *The orthonormal dual Hahn functions satisfy the following pairs of recurrence relations:*

$$\begin{aligned} & \sqrt{(n+1+\gamma)(N-n)}\tilde{R}_n(\lambda(x); \gamma, \delta, N) - \sqrt{(n+1)(N-n+\delta)}\tilde{R}_{n+1}(\lambda(x); \gamma, \delta, N) \\ &= \sqrt{x(x+\gamma+\delta+1)}\tilde{R}_n(\lambda(x-1); \gamma+1, \delta+1, N-1), \end{aligned} \quad (12)$$

$$\begin{aligned} & -\sqrt{(n+1)(N-n+\delta)}\tilde{R}_n(\lambda(x-1); \gamma+1, \delta+1, N-1) + \sqrt{(n+2+\gamma)(N-n-1)} \\ & \times \tilde{R}_{n+1}(\lambda(x-1); \gamma+1, \delta+1, N-1) = \sqrt{x(x+\gamma+\delta+1)}\tilde{R}_{n+1}(\lambda(x); \gamma, \delta, N) \end{aligned} \quad (13)$$

and

$$\begin{aligned} & \sqrt{(n+1+\gamma)(N-n+\delta)}\tilde{R}_n(\lambda(x); \gamma, \delta, N) - \sqrt{(n+1)(N-n)}\tilde{R}_{n+1}(\lambda(x); \gamma, \delta, N) \\ &= \sqrt{(x+\gamma+1)(x+\delta)}\tilde{R}_n(\lambda(x); \gamma+1, \delta-1, N), \end{aligned} \quad (14)$$

$$\begin{aligned} & -\sqrt{(n+1)(N-n)}\tilde{R}_n(\lambda(x); \gamma+1, \delta-1, N) + \sqrt{(n+2+\gamma)(N-n+\delta-1)} \\ & \times \tilde{R}_{n+1}(\lambda(x); \gamma+1, \delta-1, N) = \sqrt{(x+\gamma+1)(x+\delta)}\tilde{R}_{n+1}(\lambda(x); \gamma, \delta, N). \end{aligned} \quad (15)$$

**Proof.**

The first two relations follow from the case dual Hahn I of [17, Theorem 1] multiplied by the square root of the weight function and norm squared, and similarly the last two from the case dual Hahn III.  $\square$

**Proof of Theorem 2.**

Let  $n$  be an even integer, say  $n = 2m$ , and let  $a$  and  $b$  be real numbers greater than  $-1$ . Take  $k \in \{1, \dots, m\}$  and let  $U_{\pm k} = (u_1, \dots, u_{n+1})^T$  be the column vector with entries

$$u_l = \begin{cases} (-1)^{(l-1)/2}\tilde{R}_{(l-1)/2}(\lambda(k); \frac{a-1}{2}, \frac{b-1}{2}, m) & \text{if } l \text{ odd} \\ \pm(-1)^{l/2-1}\tilde{R}_{l/2-1}(\lambda(k-1); \frac{a+1}{2}, \frac{b+1}{2}, m-1) & \text{if } l \text{ even.} \end{cases}$$

We calculate the entries of the vector  $\tilde{H}_n(a, b)U_{\pm k}$  to be

$$(\tilde{H}_n(a, b)U_{\pm k})_l = \tilde{h}_{l, l-1}^e u_{l-1} + \tilde{h}_{l, l+1}^e u_{l+1}.$$

For  $l$  even, using the recurrence relation (12) with the appropriate parameter values substituted in the orthonormal dual Hahn functions, this becomes

$$\begin{aligned} (\tilde{H}_n(a, b)U_{\pm k})_l &= \sqrt{(l-1+a)(2m+2-l)}(-1)^{l/2-1}\tilde{R}_{l/2-1}(\lambda(k); \frac{a-1}{2}, \frac{b-1}{2}, m) \\ & \quad + \sqrt{l(2m+1-l+b)}(-1)^{l/2}\tilde{R}_{l/2}(\lambda(k); \frac{a-1}{2}, \frac{b-1}{2}, m) \\ &= 2\sqrt{k(k+\frac{a}{2}+\frac{b}{2})}(-1)^{l/2-1}\tilde{R}_{l/2-1}(\lambda(k-1); \frac{a+1}{2}, \frac{b+1}{2}, m-1) \\ &= \pm\sqrt{(2k)(2k+a+b)} u_l. \end{aligned}$$

Similarly, for  $l$  odd we have, using now the recurrence relation (13),

$$\begin{aligned} (\tilde{H}_n(a, b)U_{\pm k})_l &= \pm\sqrt{(l-1)(2m+2-l+b)}(-1)^{(l-3)/2}\tilde{R}_{(l-3)/2}(\lambda(k-1); \frac{a+1}{2}, \frac{b+1}{2}, m-1) \\ & \quad \pm\sqrt{(l+a)(2m+1-l)}(-1)^{(l-1)/2}\tilde{R}_{(l-1)/2}(\lambda(k-1); \frac{a+1}{2}, \frac{b+1}{2}, m-1) \\ &= \pm 2\sqrt{k(k+\frac{a}{2}+\frac{b}{2})}(-1)^{(l-1)/2}\tilde{R}_{(l-1)/2}(\lambda(k); \frac{a-1}{2}, \frac{b-1}{2}, m) \\ &= \pm\sqrt{(2k)(2k+a+b)} u_l. \end{aligned}$$

Finally, define  $U_0 = (u_1, \dots, u_{n+1})^T$  as the column vector with entries

$$u_l = \begin{cases} (-1)^{(l-1)/2}\tilde{R}_{(l-1)/2}(\lambda(0); \frac{a-1}{2}, \frac{b-1}{2}, m) & \text{if } l \text{ odd} \\ 0 & \text{if } l \text{ even.} \end{cases}$$

Putting  $x = 0$  on the right-hand side of (12), it is clear that the entries of the vector  $\tilde{H}_n(a, b)U_0$  are all zero.





$H_n(a, b)$  with those computed using the inherent MATLAB function `eig()`. These numerical experiments are included merely to illustrate the potential use of the matrices  $H_n(a, b)$  as eigenvalue test matrices, and to examine the sensitivity of the computed eigenvalues on the new parameters.

A measure for the accuracy of the computed eigenvalues is the relative error

$$\frac{\|x - x^*\|_\infty}{\|x\|_\infty},$$

where  $x$  is the vector of eigenvalues as ordered list (by real part) and  $x^*$  its approximation.

Recall that both for  $n$  odd and  $n$  even, for the special case  $H_n(a)$  the square roots in the expressions for the eigenvalues cancel, yielding real eigenvalues for every real value of the parameter  $a$ . In the general case, the eigenvalues (6) are real when  $a + b > -2$  and those in (8) are real when  $a > -1$  and  $b > -1$  or  $a < -n$  and  $b < -n$ . A first remark is that when we compute the spectrum of  $C_n$  using `eig()` in MATLAB, eigenvalues with imaginary parts are found when  $n$  exceeds 116, but not for lower values of  $n$ . Therefore, for the extensions, we have chosen  $n = 100$  and  $n = 101$  (for the even and the odd case respectively) for most of our tests, as this gives reasonably large matrices but is below the bound of 116. We will see that in this case for the extensions, the `eig()` function in MATLAB does find eigenvalues with imaginary part for certain parameter values.

We first consider the special case (21). For  $n$  even,  $H_n(a)$  has the eigenvalues (3), which are integers independent of the parameter  $a$ . In figure 1, we have depicted the largest imaginary part of the computed eigenvalues for the matrix  $H_n(a)$  for  $n = 10$  and  $n = 100$  at different values for the parameter  $a$ . We see that outside a central region imaginary parts are found. For example, for  $H_{100}(a)$ , MATLAB finds eigenvalues with imaginary parts when  $a > 21$  or  $a < -2.5$ . Moreover, the relative error for the computed eigenvalues, shown in figures 2, increases as  $a$  approaches the region where eigenvalues with imaginary parts are found. In this latter region, the size of the relative error is of course due to the presence of imaginary parts which do not occur in the theoretical exact expression for the eigenvalues. As a reference, the relative error for  $C_{100}$  is  $3.6612 \times 10^{-5}$ , while that for  $H_{100}(20)$  is  $1.1471 \times 10^{-3}$  and  $4.9444 \times 10^{-3}$  for  $H_{100}(20.97)$ .

For  $n$  odd,  $H_n(a)$  has the eigenvalues (18), which dependent on the parameter  $a$  but are real for every real number  $a$ . Nevertheless, even for a small dimension such as  $n = 11$ , eigenvalues with (small) imaginary parts are found when  $a$  equals  $-2, -4, -6$  or  $-8$ . This produces a relative error of order  $10^{-8}$ , while for other values of  $a$  (and for the Clement matrix) the relative error is of order  $10^{-15}$ , near machine precision. For  $H_{101}(a)$ , the largest imaginary part of the computed eigenvalues is portrayed in figure 3, together with the relative error. MATLAB finds eigenvalues with imaginary parts when  $-100 \leq a < -1.5$ . These findings correspond to the region where double eigenvalues occur as mentioned in the previous section. The relative error is largest around this region and is several orders smaller when moving away from this region. As a reference, the relative error for  $C_{101}$  is  $3.6881 \times 10^{-5}$ , while that for  $H_{101}(-1.75)$  is  $1.4840 \times 10^{-3}$ . Finally, we note that eigenvalues with imaginary parts also appear when  $a$  is extremely large, i.e.  $a > 10^{10}$  or  $a < -10^{10}$ .

Next, we consider the general setting where we have two parameters  $a$  and  $b$ , starting with the case where  $n$  is even. Although the two parameters  $a$  and  $b$  occur symmetric in (6) and in the matrix (5) itself, there are some disparities in the numerical results. From the expression for the eigenvalues (6) we see that they are real when the parameters satisfy  $a + b > -2$ . However,

- when  $a$  is a negative number less than  $-2$ , MATLAB finds eigenvalues with imaginary parts for almost all values of  $b$ .
- for negative values of  $b$ , no imaginary parts are found as long as  $a + b > -2$ .
- For positive values of  $a$ , eigenvalues with imaginary parts are found when  $b$  gets sufficiently large, as illustrated in figure 4.
- For positive values of  $b$  the opposite holds: eigenvalues with imaginary parts are found when  $a$  is comparatively small, see figure 5.

In the case where  $n$  is odd, similar results hold for positive parameter values for  $a$  and  $b$ , as shown in figure 6 for example. For negative parameter values we have a different situation, as the eigenvalues (8) can become imaginary if the two factors have opposite sign. When  $a < -n$  and  $b < -n$ , the eigenvalues (8) are real again and the behavior mimics that of the positive values of  $a$  and  $b$ . The picture we get is a mirror image of figure 6.

The reason for this disparity between the seemingly symmetric parameters  $a$  and  $b$  is that the QR algorithm wants to get rid of subdiagonal entries in the process of creating an upper triangular matrix. As a consequence, the numerical computations are much more sensitive to large values of  $b$  as it resides on the subdiagonal. This is showcased in figures 4, 5 and 6. Most important is the sensitivity on the extra parameters ( $a$  or  $a$  and  $b$ ) which makes them appealing as test matrices.

It would be interesting future work if these new eigenvalue test matrices were to be used to test also numerical algorithms for computing eigenvalues designed specifically for matrices having multiple eigenvalues [8], being tridiagonal [15], or symmetric and tridiagonal [4].

## References

- [1] E.A. Abdel-Rehim, From the Ehrenfest model to time-fractional stochastic processes. *J. Comput. Appl. Math.* **233** (2009), no. 2, 197-207.
- [2] R. Bevilacqua, E. Bozzo, The Sylvester-Kac matrix space, *Linear Algebra Appl.* **420** (2009), 3331–3138.
- [3] T. Boros, P. Rózsa, An explicit formula for singular values of the Sylvester-Kac matrix, *Linear Algebra Appl.* **421** (2007), 407–416.
- [4] P. Brockman, T. Carson, Y. Cheng, T.M. Elgindi, K. Jensen, X. Zhoun, M.B.M. Elgindi, Homotopy method for the eigenvalues of symmetric tridiagonal matrices. *J. Comput. Appl. Math.* **237** (2013), no. 1, 644–653.
- [5] P.A. Clement, A class of triple-diagonal matrices for test purposes, *SIAM Review* **1** (1959), 50–52.
- [6] J.A. Cuminato, S. McKee, A note on the eigenvalues of a special class of matrices. *J. Comput. Appl. Math.* **234** (2010), no. 9, 2724-2731.
- [7] A. Edelman, E. Kostlan, The road from Kac’s matrix to Kac’s random polynomials. In Proceedings of the 1994 SIAM Applied Linear Algebra Conference (Philadelphia, 1994), J. Lewis, Ed., SIAM, pp. 503–507. 1994.
- [8] A. Galántai, C.J. Hegedűs, Hymans method revisited. *J. Comput. Appl. Math.* **226** (2009), no. 2, 246–258.
- [9] R.T. Gregory, D.L. Karney, A collection of matrices for testing computational algorithms, Tech. Rep., 1978
- [10] N. Higham, The Test Matrix Toolbox for Matlab, *Numerical Analysis Report No. 237*, University of Manchester, 1993.
- [11] B. Igel'nik, D. Simon, The eigenvalues of a tridiagonal matrix in biogeography. *Appl. Math. Comput.* **218** (2011), no. 1, 195-201.
- [12] E.I. Jafarov, N.I. Stoilova, J. Van der Jeugt, Finite oscillator models: the Hahn oscillator, *J. Phys. A: Math. Theor.* **44** (2011), 265203.
- [13] M. Kac, Random walk and the theory of Brownian motion, *Amer. Math. Monthly* **54** (1947), 369–391.
- [14] R. Koekoek, P.A. Lesky, R.F. Swarttouw, Hypergeometric orthogonal polynomials and their  $q$ -analogues, *Springer Monographs in Mathematics*, Springer-Verlag, Berlin, 2010.
- [15] K. Maeda, S. Tsujimoto, A generalized eigenvalue algorithm for tridiagonal matrix pencils based on a nonautonomous discrete integrable system. *J. Comput. Appl. Math.* **300** (2016), 134–154.
- [16] K. Nomura, P. Terwilliger, Krawtchouk polynomials, the Lie algebra  $\mathfrak{sl}(2)$ , and Leonard pairs, *Linear Algebra Appl.* **437** (2012), 345–375.
- [17] R. Oste, J. Van der Jeugt, Doubling (dual) Hahn polynomials: classification and applications, *Symmetry, Integrability and Geometry: Methods and Applications* **12** (2016), 003.



- [18] R. Oste, J. Van der Jeugt, A finite oscillator model with equidistant position spectrum based on an extension of  $\mathfrak{su}(2)$ , *J. Phys. A: Math. Theor.* **49** (2016), 175204.
- [19] J.J. Sylvester, Théorème sur les déterminants, *Nouv. Ann. Math.* **13** (1854), 305.
- [20] O. Taussky, J. Todd, Another look at a matrix of Marc Kac, *Linear Algebra Appl.* **150** (1991), 341–360.
- [21] W.C. Yueh, Eigenvalues of several tridiagonal matrices. *Appl. Math. E-Notes* **5** (2005), 66-74.

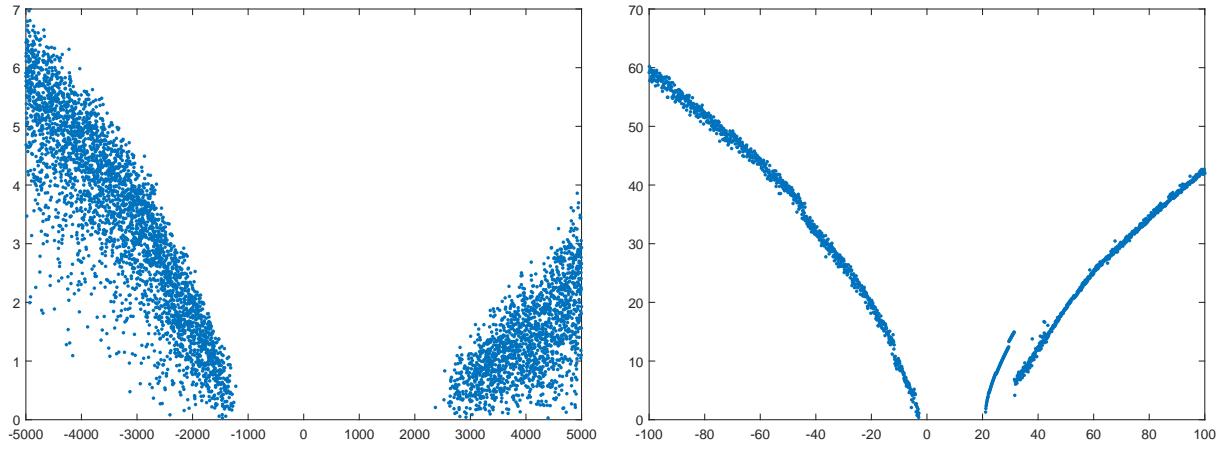


Figure 1: Plots of the largest imaginary part of the computed eigenvalues of  $H_n(a)$  ( $n$  even and  $a = -b$ ) for different values of  $a$  on horizontal axis. On the left for  $n = 10$ , on the right for  $n = 100$ .

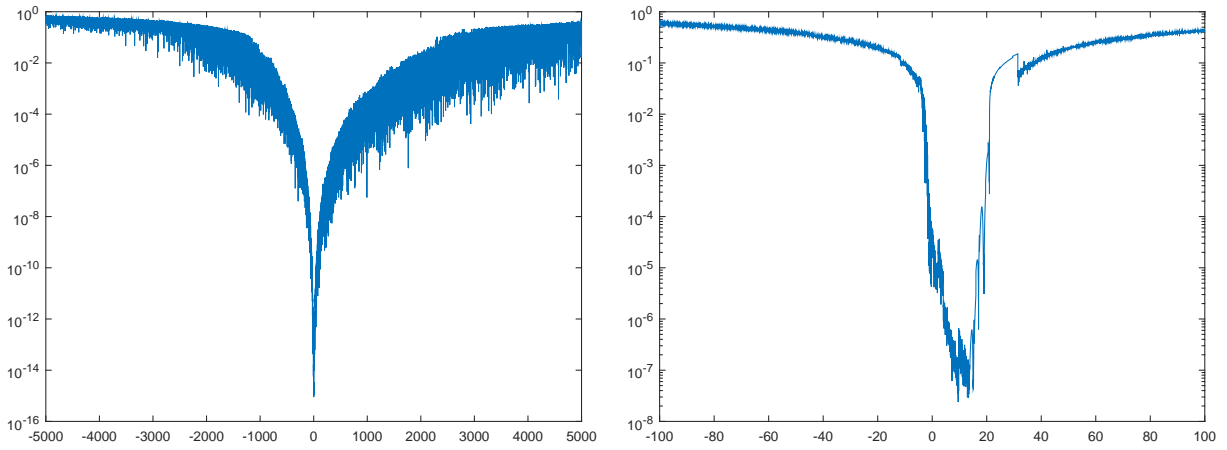


Figure 2: Plots of the relative error in the computed eigenvalues of  $H_n(a)$  ( $n$  even and  $a = -b$ ) for different values of  $a$  on horizontal axis. Left  $n = 10$  and right  $n = 100$ .

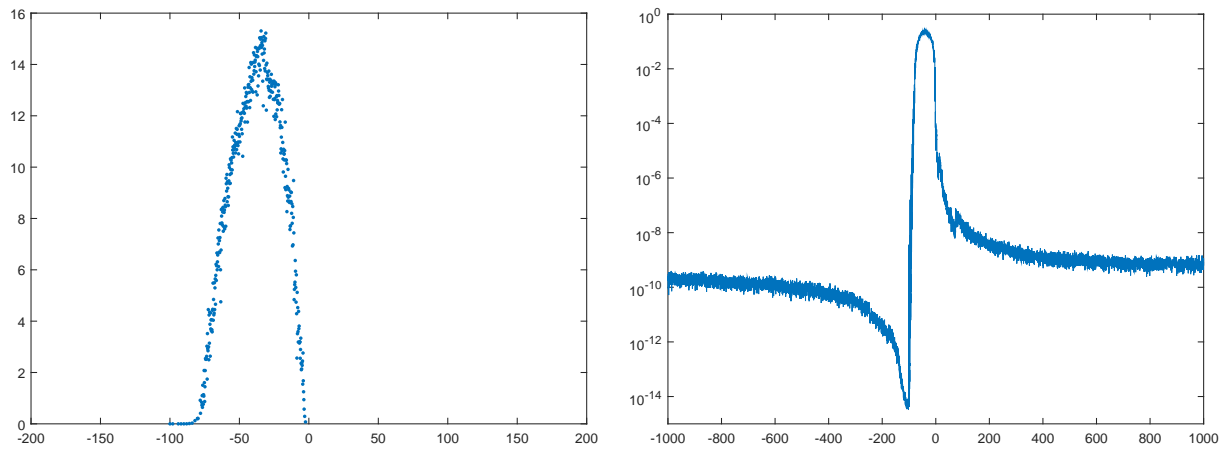


Figure 3: For different values of  $a$  as denoted on the horizontal axis, on the left a plot of the largest imaginary part and on the right a plot of the relative error of the computed eigenvalues of  $H_{101}(a)$ .

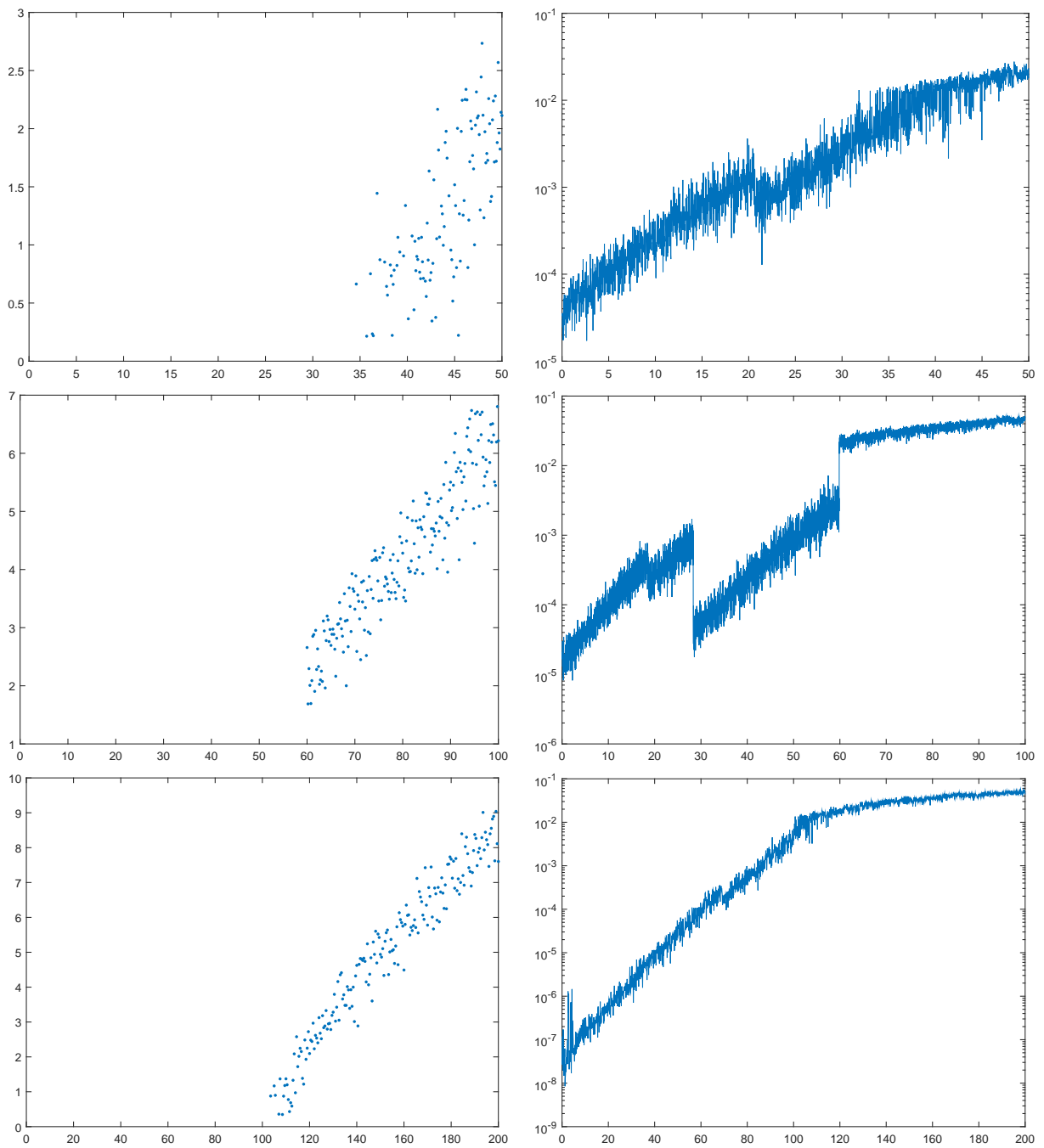


Figure 4: Plots of the largest imaginary part (left) and the relative error (right) in the computed eigenvalues of  $H_{100}(a, b)$ , horizontal axis varying values of  $b$ . Top row  $a = 0$ , middle row  $a = 1$ , bottom row  $a = 20$ .

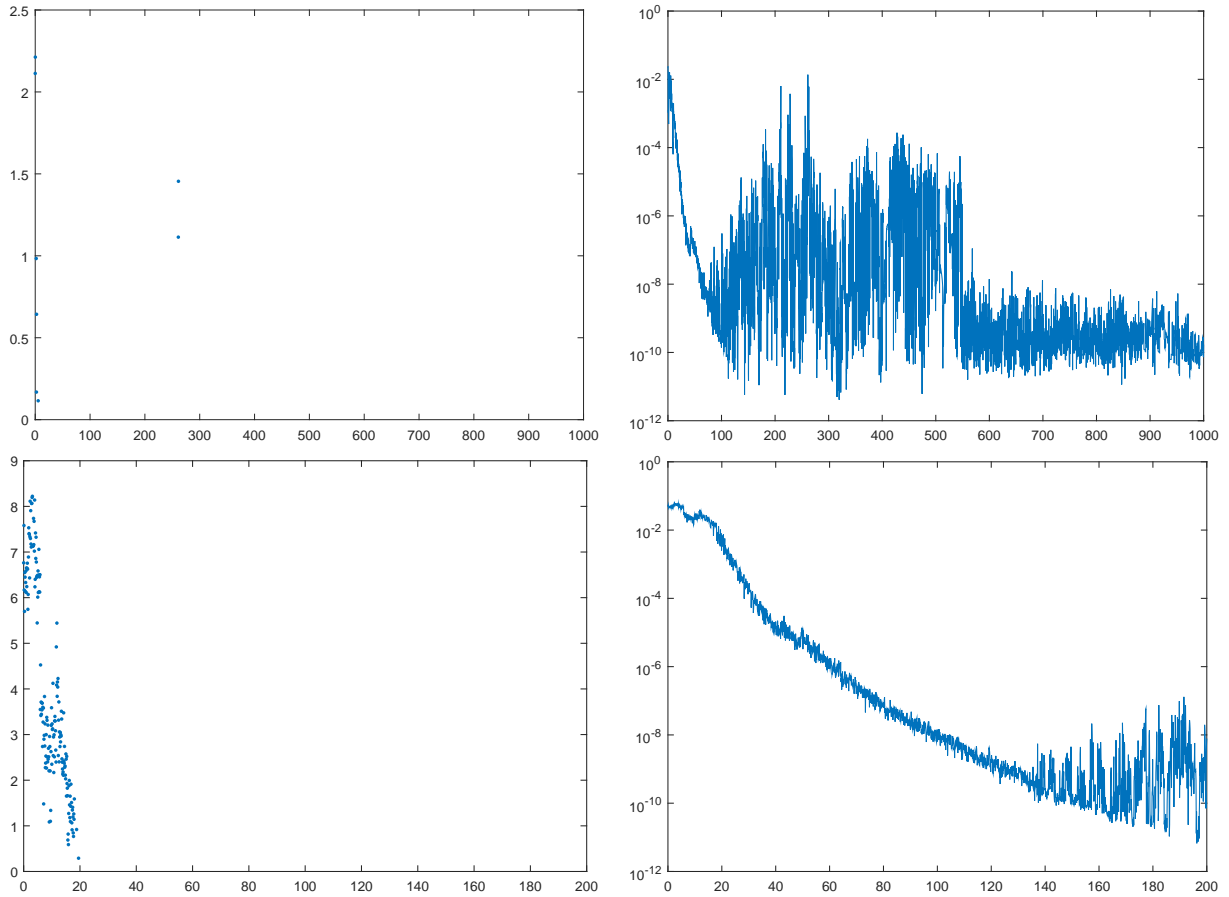


Figure 5: Plots of the largest imaginary part (left) and the relative error (right) in the computed eigenvalues of  $H_{100}(a, b)$ , horizontal axis varying values of  $a$ . Top row  $b = 50$ , bottom row  $b = 100$ .

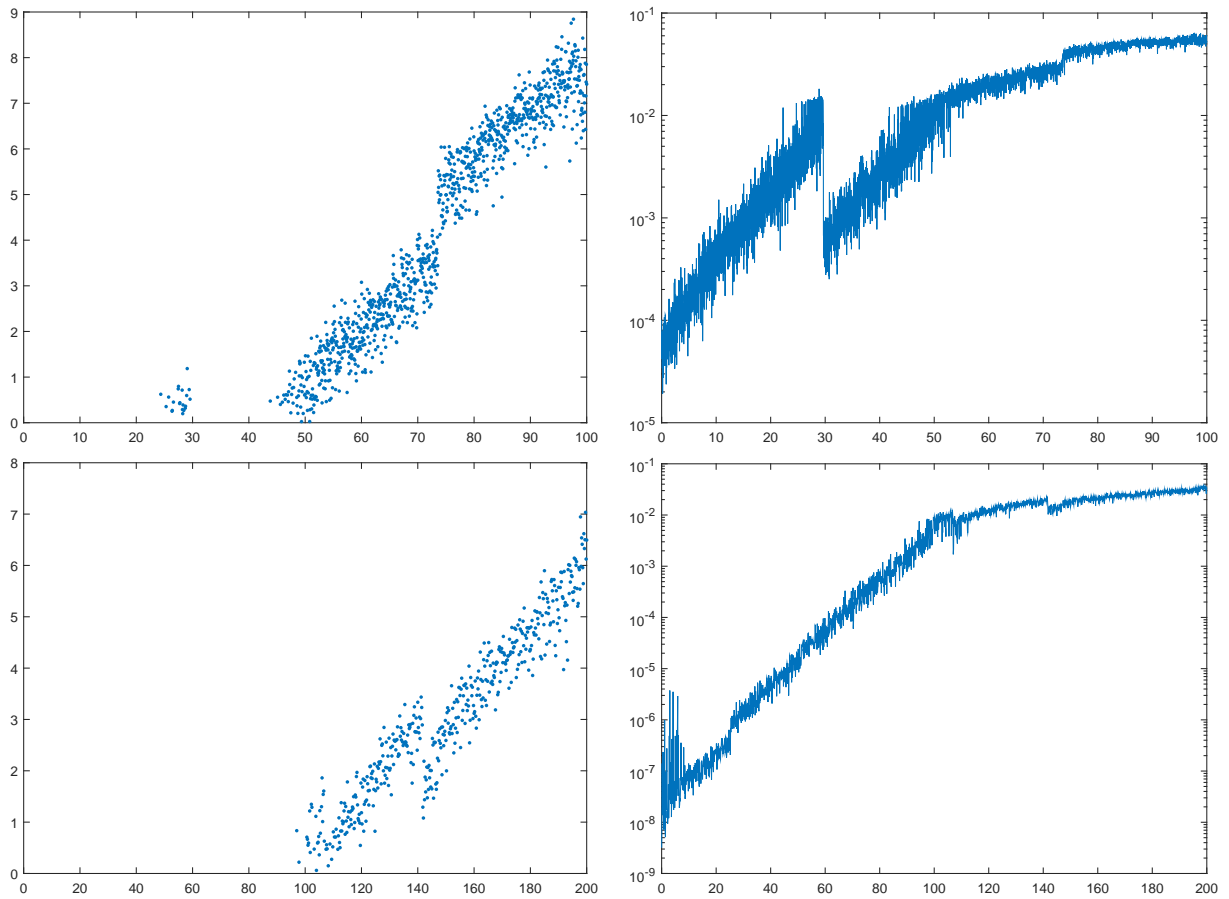


Figure 6: Plots of the largest imaginary part (left) and the relative error (right) in the computed eigenvalues of  $H_{101}(a, b)$ , horizontal axis varying values of  $b$ . Top row  $a = 0$ , bottom row  $a = 25$ .